ACS Sustainable Chemistry & Engineering

Research Article

pubs.acs.org/journal/ascecg

# Coaxial Electrospun Cellulose-Core Fluoropolymer-Shell Fibrous Membrane from Recycled Cigarette Filter as Separator for High Performance Lithium-Ion Battery

Fenglin Huang,[†] Yunfei Xu,[†] Bin Peng,[†] Yangfen Su,[†] Feng Jiang,[‡] You-Lo Hsieh,[‡] and Qufu Wei*[,†]

[†]Key Laboratory of Eco-Textiles, Ministry of Education, Jiangnan University, Wuxi 214122, China

[‡]Fiber and Polymer Science, University of California, Davis, Davis, California 95616, United States

**ABSTRACT:** This paper reports an eco-friendly approach for extracting cellulose acetate (CA) from waste cigarette filter to construct a cellulose-based membrane separator for a high-performance lithium-ion battery. A cellulose/poly(vinylidene fluoride-*co*-hexafluoropropylene (PVDF-HFP) nanofiber membrane was prepared by coaxial electrospinning of a cellulose acetate core and PVDF-HFP shell, then hydrolyzed by LiOH. The cellulose-core/PVD-HFP-shell fibrous membrane shows good tensile strength (34.1 MPa), high porosity (66%), excellent thermal stability (to 200 °C), and super electrolyte compatibility (355% electrolyte uptake). It has a lower interfacial resistance (98.5 Ω) and higher ionic conductivity (6.16 mS $cm^{-1}$) than those of commercial separators (280.0 Ω and 0.88 mS $cm^{-1}$). In addition, the rate capability (138 mAh·$g^{-1}$) and cycling performance (75.4% after 100 cycles) are also superior to those of the commercial separators, demonstrating the cellulose-core fibrous membrane to be a promising separator for a high-power and more secure lithium-ion battery.

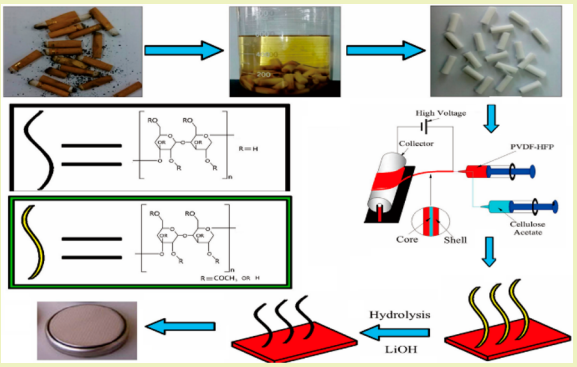


**KEYWORDS:** *Coaxial electrospinning, Separator, Recycled cellulose*

## INTRODUCTION

Lithium-ion batteries (LIBs) with high specific energy and long cycle lifetime are highly desirable because of their wide applications in every expanding use of smart electronic devices, portable electronics, and electric vehicles.[1−4] At the same time, the development of sustainable energy devices has attracted increasing attention due to environmental pollution and exhausted fossil fuel.[5] However, various safety issues of LIBs, with internal short-circuits being one of the most critical threats, are difficult to avoid. A separator in LIBs is a key component to prevent such failures, because it can isolate the cathode and anode, to prevent electrical short-circuits, while allowing rapid transport of ionic charge carriers.[6,7]

Commercial separator materials used in LIBs are polyolefins, for their superior electrochemical stability and considerable mechanical strength.[8,9] However, due to their nonpolar nature, these materials show poor liquid electrolyte retention and do not absorb electrolytes with high dielectric constants, such as cyclic carbonates.[10] These disadvantages lead to lower ionic conductivity and higher electrolyte leakage. Therefore, more polar and higher ionic conductive polyvinylidene fluoride (PVDF) and its copolymer, poly(vinylidene fluoride-*co*-hexafluoropropylene) (PVDF-HFP), have received special attention as promising host polymers for separators in LIBs.[11−13] However, PVDF and PVDF-HFP separators also have their disadvantages, such as the inferior thermal stability due to their low softening or melting behavior,[14,15] making it difficult to serve the critical function of electronic isolation between cathode and anode in large-sized batteries at elevated temperatures or under vigorous conditions. A few studies have pointed out that poor liquid electrolyte retention due to their intrinsically hydrophobic character would restrict applications in high performance lithium-ion batteries.[16,17]

More recent attention has been drawn to the use of renewable polymers. A cellulose-based membrane could be a promising LIB separator due to its super thermal stability and hydrophilic property. Cellulose-based materials have found massive industrial applications, with most being disposed after usage, such as the cellulose acetate cigarette filter, posing severe environmental threat. Therefore, recycling a cellulose acetate cigarette filter and applying it as a LIB separator not only alleviates environmental pressure but also produces more value-added products. To generate high quantities of fine pores desirable for lithium-ion diffusion to perform the charge−discharge behavior while with excellent physical integrity, a network of ultrafine and nanoscale fibers produced by electrospinning is a viable option.[18,19] Our group has proved that coaxial electrospinning is a simple and low-cost approach to achieve core/shell nanofibers, and the core/shell structure can be manipulated by selectively adjusting solution properties

Received: January 15, 2015
Revised: March 15, 2015
Published: March 25, 2015

  

DOI: 10.1021/acssuschemeng.5b00032
*ACS Sustainable Chem. Eng.* 2015, 3, 932−940

**Scheme 1. Preparation Process of Cellulose-based Coaxial Nanofiber Separators for Lithium-Ion Battery**

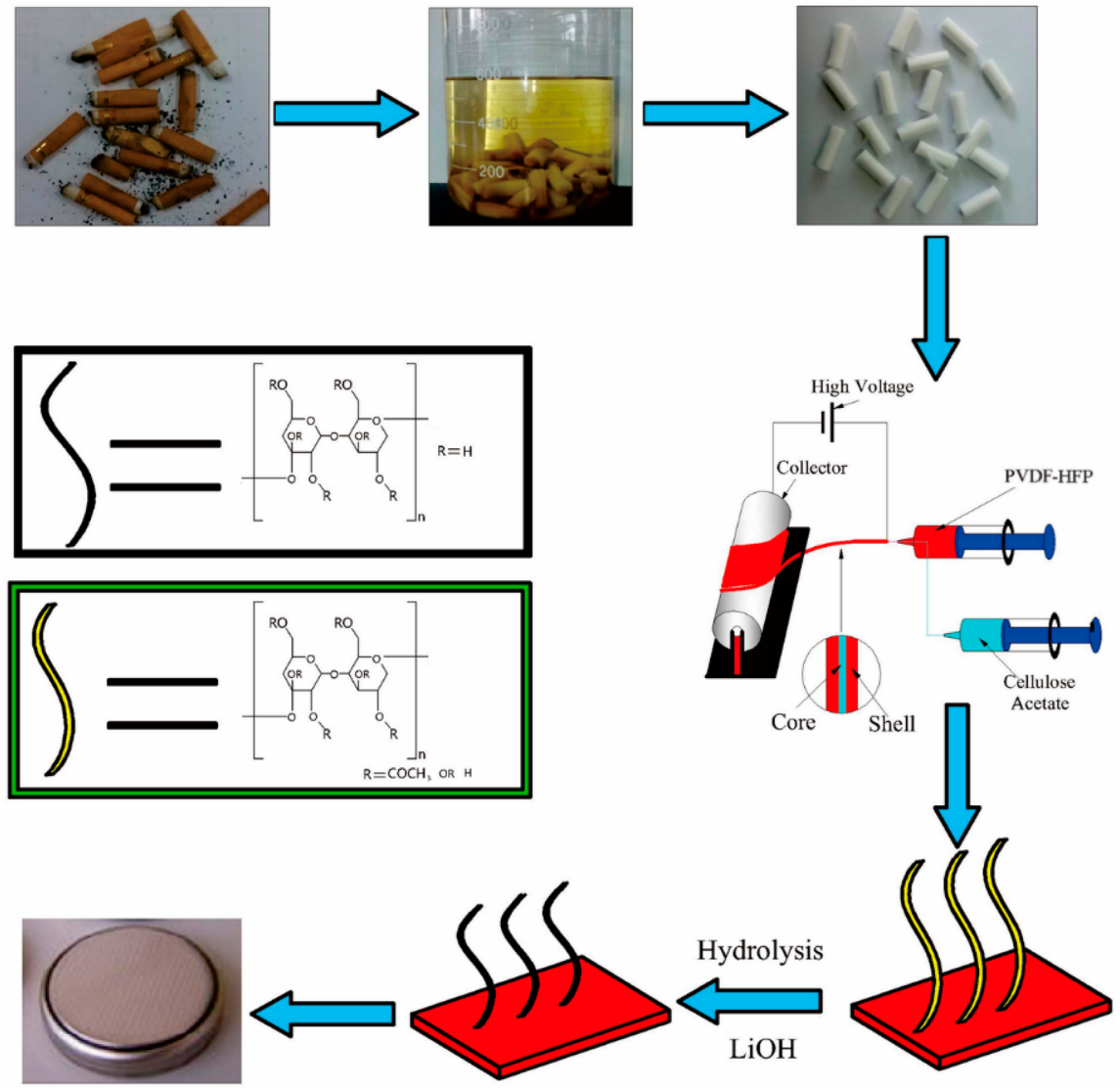


and operating parameters.[20] Here, cellulose acetate was extracted and purified from waste cigarette filter tips, and was coaxially electrospun with PVDF-HFP to prepare a cellulose-based core/shell nanofiber membrane. The thermal stability and hydrophilicity were further improved by converting cellulose acetate to cellulose via LiOH hydrolysis. The environmentally friendly, cost-effective, good mechanical property, super thermal stability, and excellent electrochemical properties of this cellulose-based coaxial nanofiber membrane would endow it as a very promising separator for high performance lithium-ion batteries.

## EXPERIMENTAL SECTION

Poly(vinylidene fluoride-*co*-hexafluoropropylene) (PVDF-HFP) (Mw 50 kDa) was purchased from Shanghai 3F New Materials Co., Ltd. (Shanghai, China). The commercial separator (PP, 2300) was supplied by Celgard LLC. Dimethylacetamide (DMAc) and acetone were supplied by Sinopharm Chemical Reagent Co., Ltd. (Shanghai, China) and used without further purification. Waste cigarette filter tips were collected from ashtrays at Jiangnan University. The wrapping paper and any remaining tobacco and chars were manually removed from the cigarette tips first. The cellulose acetate filters were soaked in distilled water at room temperature for 12 h, followed by sonication in ethanol for 5 h with a UP400S ultrasonicator. The washing solution was decanted, and the tips were sonicated in fresh ethanol for three times with the power of 100 W. The cleaned tips were then dried at 80 °C for 6 h prior to use. The electrolyte was composed of 1 M $LiPF_6$ dissolved in ethylene carbonate, dimethyl carbonate, and ethylene methyl carbonate (1:1:1, v/v/v).

The core and shell solutions were prepared by dissolving the extracted cellulose acetate (CA) into DMAc and acetone (2/1, w/w) to 15 wt % and PVDF-HFP in a mixture of DMAc and acetone (3/7, w/w) to 10 wt %, respectively. These solutions were independently fed through concentrically configured needles with outer and inner diameters of 1.3 and 0.3 mm, respectively (Scheme 1). Coaxial electrospinning was carried out at 15 kV with a 150 mm needle-to-collector distance and a fixed 0.9 mL/h flow rate for the PVDF-HFP solution. To obtain different core/shell morphologies, CA core and PVDF-HFP shell solutions were fed at 1:3, 2:3, and 3:3 flow rate ratios. The as-prepared electrospun nanofibers were then dried in a vacuum oven at 60 °C for 12 h. Hydrolysis of the cellulose acetate/PVDF-HFP membrane was performed in 0.05 M LiOH aqueous solution at ambient temperature for 10 h to produce a cellulose/PVDF-HFP membrane that was rinsed in distilled water and dried under vacuum at 60 °C for 12 h.

The morphology of cellulose acetate/PVDF-HFP nanofibers was observed by field emission scanning electron microscopy (FE-SEM, Hitachi) and transmission electron microscopy (TEM; JEM-2100HR,


DOI: 10.1021/acssuschemeng.5b00032
*ACS Sustainable Chem. Eng.* 2015, 3, 932−940

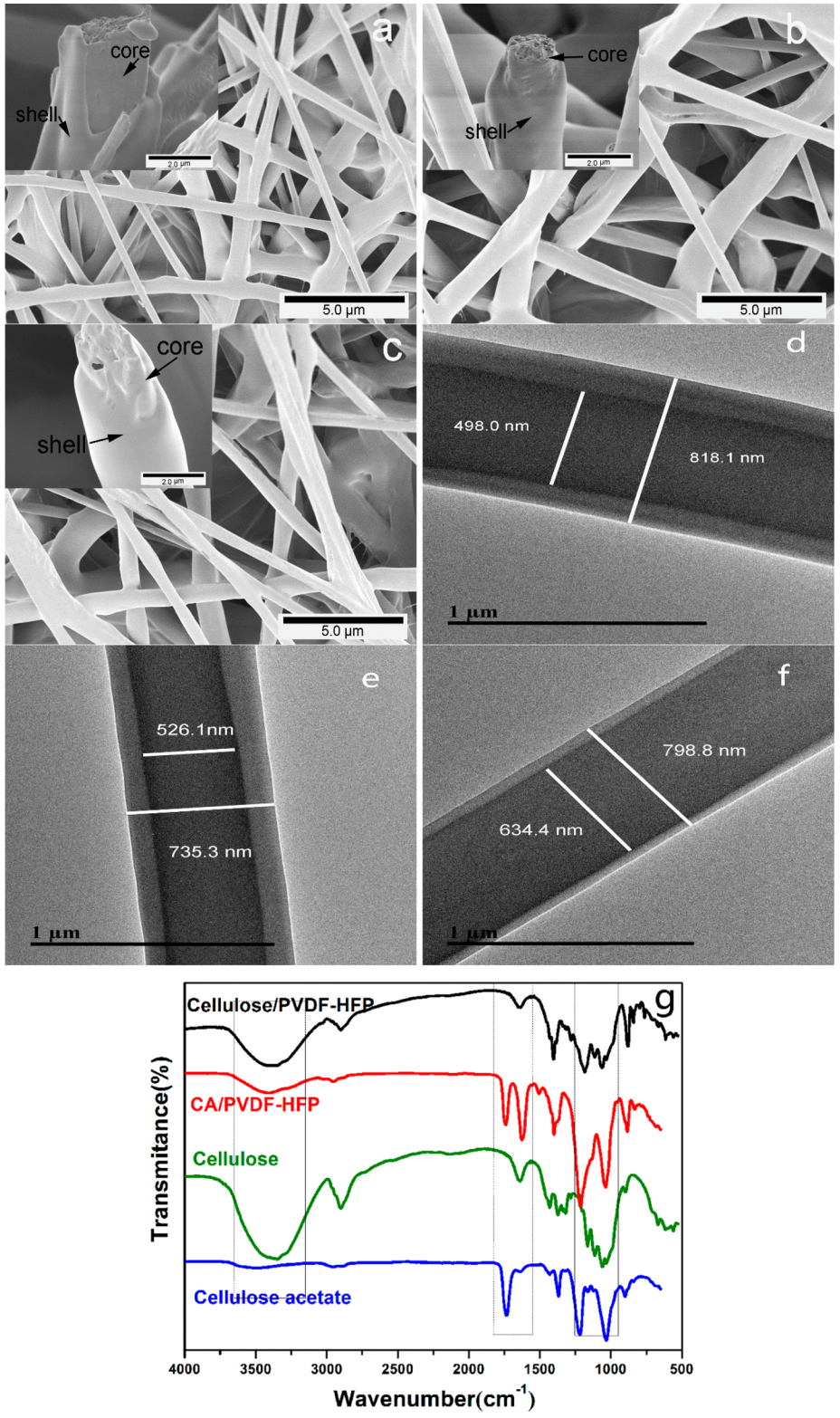


**Figure 1.** SEM (a–c) and TEM (d–f) images of coaxial CA/PVDF-HFP nanofibers with varying core/shell flow rate ratios: 1:3 (a,d), 2:3 (b,e), and 3:3 (c,f); Insets in panels a–c are SEM images of cross sections of nanofiber; FT-IR spectra of nanofiber membrane (g).

JEOL). Fiber diameter was measured from SEM images of over 50 individual fibers using PHOTOSHOP (Adobe, San Jose, CA). The cross sections of membranes for SEM observation were prepared by fracturing in liquid nitrogen. Fourier transform infrared (FT-IR) measurement was carried out on a Nicolet IS10 spectrometer. The mechanical strength was examined using KD-0.05 universal tester at a stretching speed of 1.5 $mms^{-1}$. Atomic force microscopy (AFM, CSPM 4400) was used to analyze the surface morphology of nanofibers. The membrane wettability was performed by carefully depositing a drop (5 $\mu$L) of the electrolyte on the membrane and the contact angle between membrane and liquid electrolyte was measured (DSA100, KRUSS) in 30 s. The thermal stability was evaluated by analyzing the shape change of separators after heating at 200 °C for 1 h. Differential scanning calorimetry (DSC) of the membrane was


DOI: 10.1021/acssuschemeng.5b00032
ACS Sustainable Chem. Eng. 2015, 3, 932–940

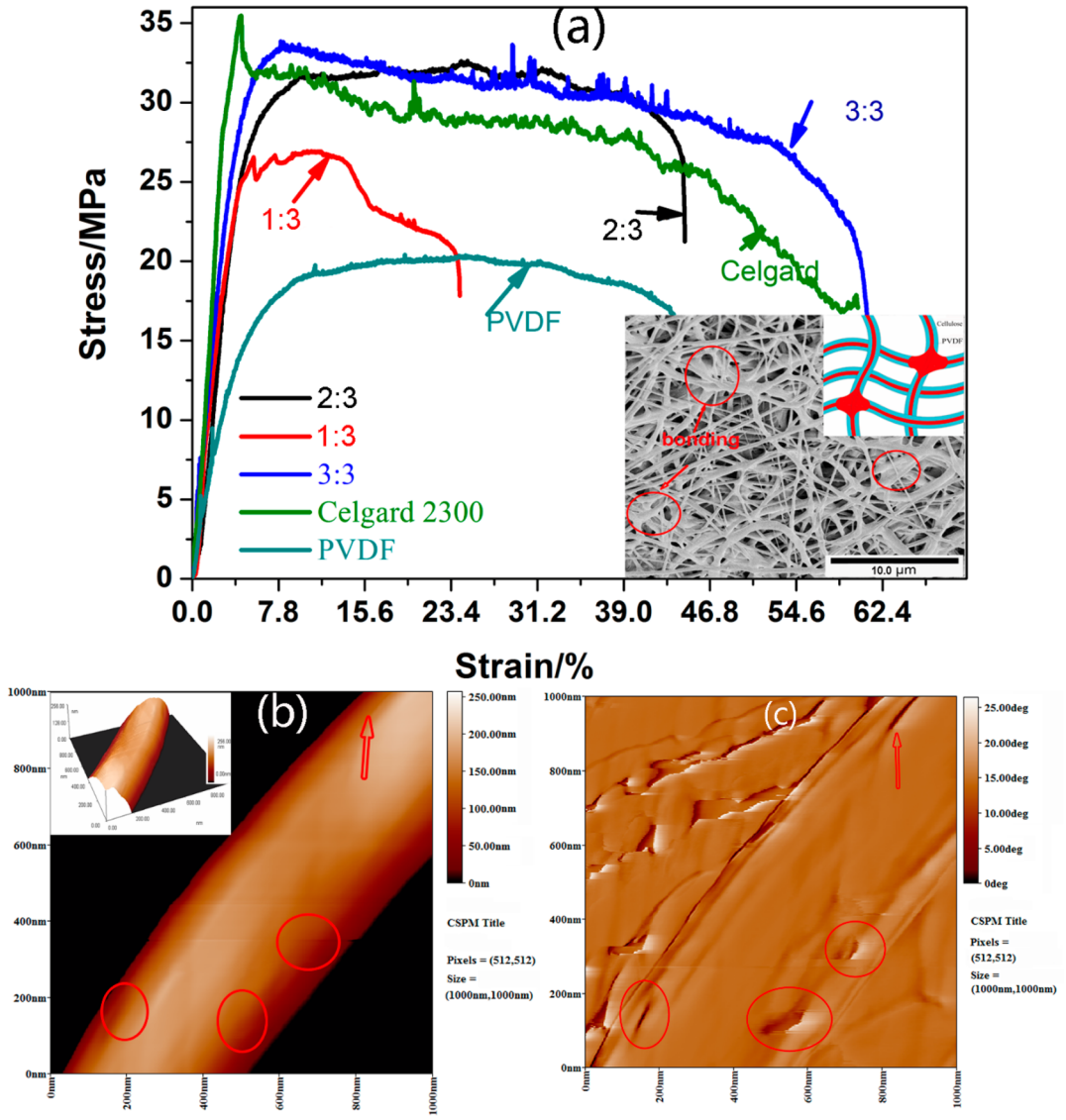


**Figure 2.** Stress–strain curves of separators (a), inset is SEM image of coaxial cellulose/PVDF-HFP nanofibers with 3:3 flow rate ratio. AFM topography (b) and phase (c) images of coaxial cellulose/PVDF-HFP nanofibers with 3:3 flow rate ratio.

carried out from 30 to 300 °C at a 10 °C/min heating rate under $N_2$ atmosphere using a TA Q200.

The separator porosity was determined by immersing the membrane in *n*-butanol for 1 h.[21] The porosity of the membrane ($P$) was calculated using the following equation:

$$P = (m_b/\rho_b)/(m_b/\rho_b + m_s/\rho_s) \times 100\% \quad (1)$$

where $m_b$ and $m_s$ are masses of *n*-butanol and the separator, $\rho_b$ and $\rho_s$ are the densities of *n*-butanol and the separator, respectively. The electrolyte uptake ($\eta$) was calculated by the weight of separator before ($W_0$) and after ($W$) soaking in liquid electrolyte for 2 h as

$$\eta = [(W - W_0)/W_0] \times 100\% \quad (2)$$

The excess *n*-butanol or electrolyte solution on the separator surfaces was absorbed with a filter paper before measuring the weight.

The testing cells had a typical three-electrode construction using lithium foils as both the counter electrode and reference electrode. The cells were assembled in an argon-filled glovebox. Charge–discharge tests were carried out at a current density from 0.2–5.0 C in a range of 2.8–4.2 V versus $Li/Li^+$, all at 20 °C. The commercial separator (Celgard 2300) was assembled and tested the same way. The interfacial resistances between two lithium plates were investigated by electrochemical impedance spectroscopy (EIS) measurement. The ionic conductivity of cellulose-based and reference separator were evaluated using EIS measurement in combination with an Electrochemical Workstation (CHENHUA, CHI710b). The electrochemical stability of the separators was measured by a linear sweep voltammograms (LSV) on a stainless-steel working electrode and a lithium metal counter electrode at the potential range between 2.5 and 6.0 V under the scan rate of 1.0 $mV \cdot s^{-1}$ at 20 °C.

## RESULTS AND DISCUSSION

The cellulose acetate/PVDF-HFP core–shell nanofibers were fabricated by coaxially electrospining 15% cellulose acetate and 10% PVDF-HFP core and shell solutions, respectively. The fibers electrospun from the three varying core and shell solution flow rate ratios appeared similar, as shown in Figures 1a–c. The fibers coaxially electrospun at 1:3, 2:3, and 3:3 core-to-shell solution flow rates were averaged as 692 ± 127 nm, 710 ± 198 nm (Figure 1b), and 689 ± 138 nm (Figure 1c) in diameter, respectively, showing statistically insignificant variations among all three samples. Compared with CA/PVDF-HFP nanofibers (Figure 1c), hydrolyzed nanofibers (Figure 2a, inset) exhibited a similar smooth surface morphology with a diameter of about



DOI: 10.1021/acssuschemeng.5b00032
*ACS Sustainable Chem. Eng.* 2015, 3, 932–940

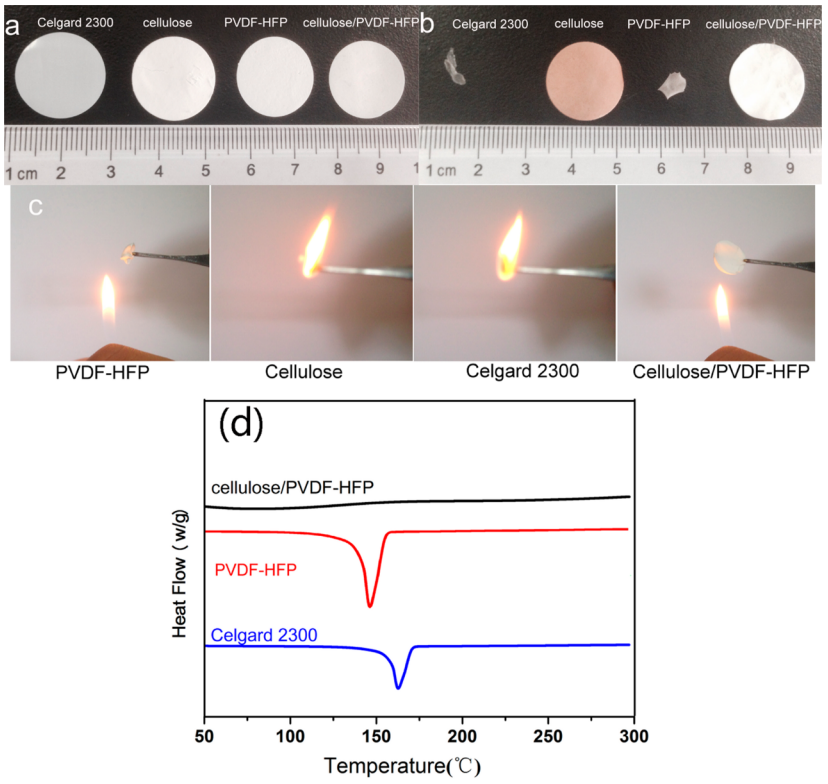


**Figure 3.** Photographs of the separators before and after thermal treatment in an oven at 200 °C for 1 h (a,b), combustion photos (c), and DSC curves (d) of various separators.

690 nm. The fractured ends of fibers from the three membranes showed clear core−shell structures with apparently different core and shell thicknesses (inset in Figure 1a−c), consistent with the biphasic darker cellulose acetate cores and lighter PVDF-HFP shells in the TEM images (Figure 1e−g). As the relative core to shell solution flow rate ratio increased, the shell became proportionally thinner, indicative of an increased cellulose acetate core. The fractions of core to overall fiber diameter increased from 0.61, 0.72, and 0.79 at 1:3, 2:3, and 3:3 flow rate ratios, respectively, very close to their respective theoretical values of 0.58, 0.71, and 0.78 calculated from core and shell flow rate ratios. Both SEM and TEM images confirmed that coaxially electrospinning of CA and PVDF-HFP solutions was effective in generating similarly sized core−shell fibers with core−shell proportions controllable by the respective solution flow rates. FTIR spectra of CA/PVDF-HFP membrane, and cellulose/PVDF-HFP membrane were used to monitor the chemical structural changes from alkaline hydrolysis (Figure 1g). The CA/PVDF-HFP spectra showed a small shoulder at 1200 $cm^{-1}$ and a prominent peak at 1425 $cm^{-1}$, characteristic C—F and C—H wagging peaks from PVDF-HFP, respectively. The presence of cellulose acetate in CA/PVDF-HFP was confirmed by the sharp peak at 1730 $cm^{-1}$ from the carbonyl (C═O) stretching of acetate, as well as the shoulder at 1374 $cm^{-1}$ and a major peak at 1238 $cm^{-1}$, ascribed to the C—H bond in $-O(C{=}O)-CH_3$ and −CO− stretching of the acetyl group, respectively. After alkaline hydrolysis, the carbonyl stretching peak (1730 $cm^{-1}$) completely disappeared, along with the disappearance of the peaks at 1374 and 1238 $cm^{-1}$, indicating successful conversion of cellulose acetate to cellulose. This conversion was further confirmed by the increased O—H stretching vibration at 3300 to 3500 $cm^{-1}$, indicating the hydrolyzing acetate groups to hydroxyls.

The stress−stain curves of cellulose/PVDF-HFP membranes electrospun at varying flow rate ratios are depicted in Figure 2a, along with electrospun PVDF-HFP membrane and commercial separator Celgard 2300 for comparison. The cellulose/PVDF-HFP separator electrospun at 3:3 flow rate ratio exhibited a maximum stress of 34.1 MPa, close to the 35.9 MPa for the commercial separator, but a distinctly different stress−strain behavior. The Celgard 2300 curve displays a typical characteristic stress−stain curve of the nanofiber membrane, showing a sharp stress drop after reaching the maximum stress point. In contrast, the cellulose/PVDF-HFP curves declined steadily after the maximum stress point with a plateau on the stress−stain curve, indicating no abrupt breakage under stress. The maximum stress of all three coaxially electropun cellulose/PVDF-HFP membranes were higher than that of pure PVDF-HFP separator (20 MPa) with similar appearance, diameter and thickness, confirming the reinforcing contribution of cellulose. The maximum stress of the three cellulose/PVDF-HFP membranes also increased from 27 to 32.4 and 34.1 MPa with increasing cellulose contents of 61, 72, and 79%, respectively, reaffirming the role of cellulose in improving the membrane strength. It has been indicated that the bonding point between fibers could enhance the mechanical property of the fiber membrane. In the cellulose/PVDF-HFP composite, cellulose is easier to form a bonding point during electrospinning due to the abundant polar groups; therefore, topography and phase images of the cellulose/PVDF-HFP nanofibers electrospun at 3:3 flow rate ratios are shown in Figure 2b,c. The topography images showed a smooth surface with occasional convex shapes on the surface of the nanofiber (circled and arrowed in Figure 2b,c), which showed more


DOI: 10.1021/acssuschemeng.5b00032
ACS Sustainable Chem. Eng. 2015, 3, 932−940

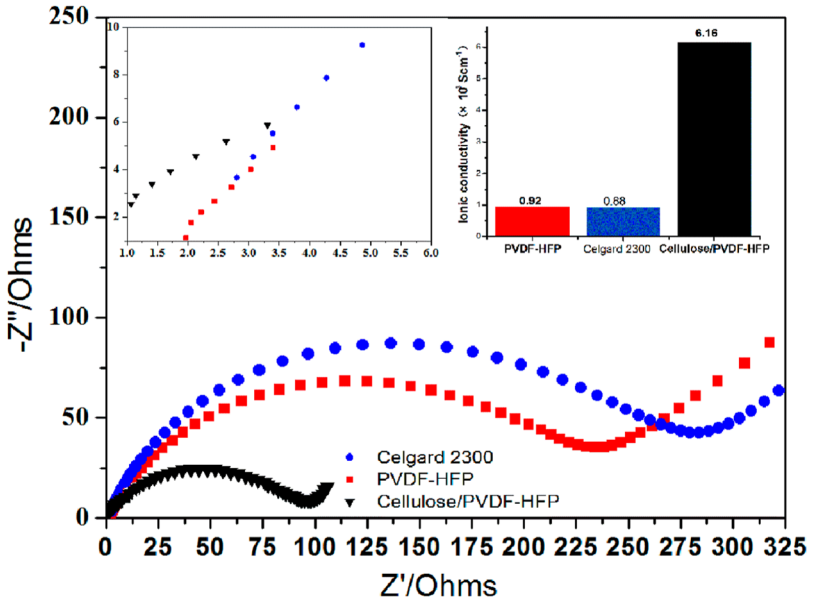


**Figure 4.** Nyquist plots of Li/electrolyte-soaked separator/Li cells at 20 °C; insets are magnified Nyquist plot and ionic conductivity of separators.

obvious contrast in the phase image, possibly suggesting biphasic surface morphologies due to the different properties of cellulose and PVDF-HFP. Consequently, it could be deduced from AFM images that a compound with a different composition (PVDF-HFP and cellulose) is formed on the surface of the nanofiber, which could be due to the diffusion of cellulose into the PVDF-HFP phase, considering the thinner shell structure at higher flow rate ratio. Considering its better mechanical property, cellulose/PVDF-HFP membrane coaxially electropsun from the 3:3 flow ratio was chosen for thermal and electrochemical investigation.

Thermal stability is an important property for a separator in LIB applications. The photographs of the separators before and after thermal treatment in an oven at 200 °C for 1 h are shown in Figure 3a,b. The PVDF-HFP nanofiber membrane shows an apparent shrinkage after heating, whereas the pure cellulose nanofiber membrane shows no shrinkage, but rather, a browning effect. However, the coaxial cellulose/PVDF-HFP membrane exhibits negligible dimensional change and color variation, manifesting its excellent thermal dimensional stability, much superior to the commercial separator (Celgard 2300) with significant shrinkage (85%) upon heating to 200 °C.

The ability of the separators to resistant or retain their physical integrity to an open flame is another important factor related to the safety of the LIBs. Upon exposure to a flame, both the Celgard 2300 and cellulose membrane separators immediately catch on fire in less than 2 s. Although the PVDF-HFP membrane shows a good flame retarding ability without catching fire, severe shrinkage was observed, consistent with its response to heat, as shown previously. In contrast to the burning or severe shrinkage, the cellulose/PVDF-HFP separator showed the best flame retarding ability and dimensional stability, which could be attributed to the core−shell structure, with the flame retarding PVDF-HFP shell and the thermally stable cellulose core. Thermal shrinkage of commercial separator at high temperature could cause internal short-circuits, and more seriously, lead to fire outbreaks and even explosions. The superior dimensional stability of cellulose-based coaxial nanofiber membrane should be beneficial to enhance safety characteristics of lithium-ion batteries.

DSC measurement is employed to further investigate the thermal stability of separators (Figure 3d). The Celgard 2300 separator starts to melt at 150 °C and shows an endothermic peak at 161.8 °C, corresponding to its melting point. Though the heating curve of PVDF-HFP shows a low melting peak at 146.4 °C, the curve of the cellulose/PVDF-HFP composite does not show any obvious endothermic peak below 300 °C, indicating better thermal stability than the Celgard separator, due to the core cellulose material, which does not melt, but rather, decomposes above 300 °C. The results showed that at temperatures above 161.8 °C, LIBs assembled with cellulose/PVDF-HFP are safer than that with Celgard 2300 separators.

It is well-known that ionic conductivity and interfacial compatibility are the two key factors that affect the electrochemical performance of separators.[22−24] The Nyquist plots of the liquid electrolyte-soaked separators and a lithium metal anode are characterized by electrochemical impedance spectroscopy and shown in Figure 4. It is well-known that the semicircle at the high frequency zone represents the charge-transfer resistance accompanied by migration of the lithium ions between the electrode and electrolyte interface.[25] The straight sloping line corresponds to the diffusion of lithium ions in the active material of the electrode. It can be seen from Figure 4 that the interfacial resistance values are 98.5, 280, and 235 Ω for cellulose/PVDF-HFP, Celgard 2300, and PVDF-HFP membrane separators, respectively. Obviously, the interfacial property between the anode and separator can be significantly improved in the case of the cellulose/PVDF-HFP separator, indicating better interfacial compatibility with the electrode material. The lower charge-transfer resistance is related to the higher electrolyte uptake and better interface compatibility, which are beneficial to improve cycle performance and rate capability. Table 1 shows the contact angle, porosity, and electrolyte uptake of Celgard 2300, cellulose/PVDF-HFP, cellulose, and PVDF-HFP membranes. The contact angle between separator and electrolyte is known to correlate to electrolyte uptake. The contact angles of the Celgard 2300 separator and PVDF-HFP membrane are 69° and 55°, leading to low electrolyte uptakes of 140 and 242%, respectively. Both cellulose and cellulose/PVDF-HFP mem-


DOI: 10.1021/acssuschemeng.5b00032
ACS Sustainable Chem. Eng. 2015, 3, 932−940

**Table 1. Porosity, Electrolyte Uptake, and Contact Angle of Separators**

| sample | porosity (%) | electrolyte uptake (%) | contact angle (deg) |
|---|---|---|---|
| Celgard 2300 | 47.88 | 140% | 69.29 |
| cellulose | 69.69 | 397% | |
| PVDF-HFP | 62.33 | 242% | 55.38 |
| cellulose/PVDF-HFP | 66.36 | 355% | |

branes immediately absorb electrolyte upon contact to 397 and 355% due to the hydrophilic nature of cellulose, making it impossible to measure the contact angle, suggesting the better interfacial compatibility between the separator and electrolyte. Besides interfacial compatibility, separator porosity is another critical factor for electrolyte uptake.[25] The porosity of the cellulose/PVDF-HFP nanofiber membrane (66%) is fairly higher than that of the Celgard 2300 separator (48%). Both the better wettability and higher porosity of the cellulose-based coaxial membrane lead to the higher electrolyte uptake of 355%, ca. 154% and 47% higher than those of the Celgard 2300 separator (140%) and PVDF-HFP nanofiber membrane (242%).

The electrochemical stabilities of the cellulose/PVDF-HFP separator and other reference separators were evaluated by observing linear sweep voltammograms and their corresponding voltammogram (Figure 5). It can be seen from the voltammogram that the decomposition voltage of the cellulose nanofiber membrane is around 3.8 V versus Li/Li$^+$, indicating this separator exhibited poor anodic stability. This phenomenon could be ascribed to the poor interfacial compatibility between the separator and electrolyte. However, no appreciable decompositions of PVDF-HFP and cellulose/PVDF-HFP separators were observed below 5.0 V versus Li/Li$^+$, which is almost comparable to that of the Celgard 2300 separator. This result demonstrates the good electrochemical stability of the cellulose/PVDF-HFP separator as a promising alternative to the commercial separator for high-voltage lithium-ion batteries.

The electrochemical properties of the cellulose/PVDF-HFP separator are investigated by charge and discharge testing and cycling performance characterization (Figure 6). The discharge capacity of batteries assembled with cellulose/PVDF-HFP is around 138 mAh·g$^{-1}$ at 0.2 C, approximately 20% higher than the 114.8 mAh·g$^{-1}$ discharge capacity for the Celgard 2000 separators, and is also superior to those references listed in Table 2.

The improved electrochemical performance of the cellulose/PVDF-HFP separator could be due to the increased ionic conductivity and transference number of Li$^+$ ions. As another important parameter for rating LIBs, the cycling stability of the $LiCoO_2$ cells using either the Celgard 2300 or cellulose/PVDF-HFP separator at 0.2 C/0.2 C was tested for up to 100 cycles (Figure 6a). The discharge capacity for the cell with Celgard 2300 maintained over 102.6 mAh·g$^{-1}$ after 40 cycles, then dropped rapidly to 30.1 mAh·g$^{-1}$, with a final retention ratio of only 27.28%. However, the cell with the cellulose/PVDF-HFP separator shows better cycling performance with minimal discharge capacity fading up to 80 cycles, then gradual fading to a high discharge capacity of 105.8 mAh·g$^{-1}$ or 75.4% retention ratio after 100 cycles, far superior than most commercial separators that only have discharge retention ratios of 61% after 100 cycles.[30] The corresponding charge−discharge curves for some selected cycle numbers are shown in Figure 6b,c. It is clear that the discharge capacity fading for the Celgard 2300 cell was severe after 50 cycles, whereas that for the cellulose/PVDF-HFP cell was minimal. With increased current densities of 0.2, 0.5, 1, 2, and 5 C, the discharge capacities decrease from 138 to 121, 104.1, 96, 62, and 32.9 mAh·g$^{-1}$ for the cellulose/PVDF-HFP cells, respectively; nevertheless, all much higher than the respective 114.8, 94.5, 72.8, 83, 32, and 12.9 mAh·g$^{-1}$ for the Celgard 2300 cells. The superior discharge capacity and cycling performance could be ascribed to the higher ionic conductivity and better interfacial compatibility of the electrolyte-soaked cellulose/PVDF-HFP nanofiber membrane. Considering the excellent discharge capacity and cycling performance as well as the aforementioned better thermal dimensional stability, the

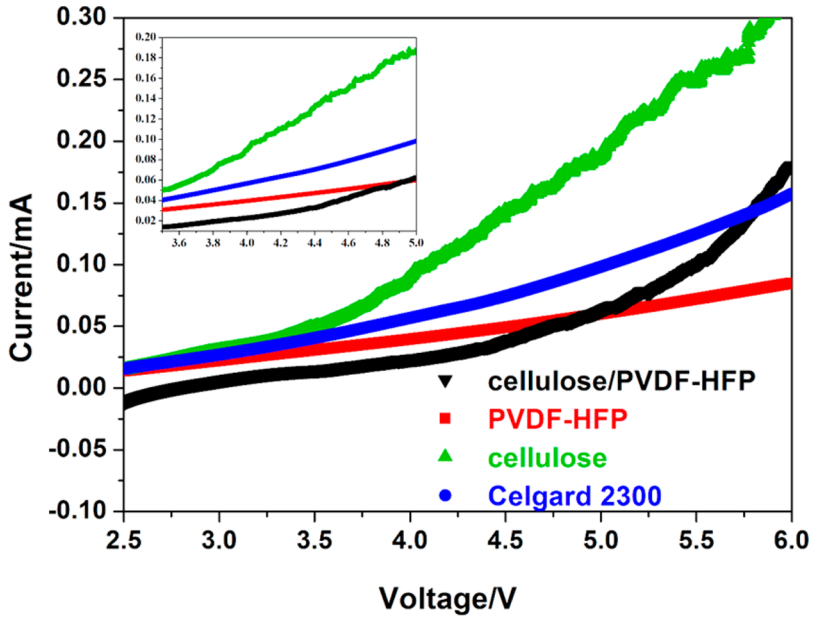


**Figure 5.** Linear sweep voltammogram curve of Celgard 2300, cellulose, PVDF-HFP, and cellulose/PVDF-HFP at a scan rate of 1.0 mV s$^{-1}$.



DOI: 10.1021/acssuschemeng.5b00032
ACS Sustainable Chem. Eng. 2015, 3, 932−940

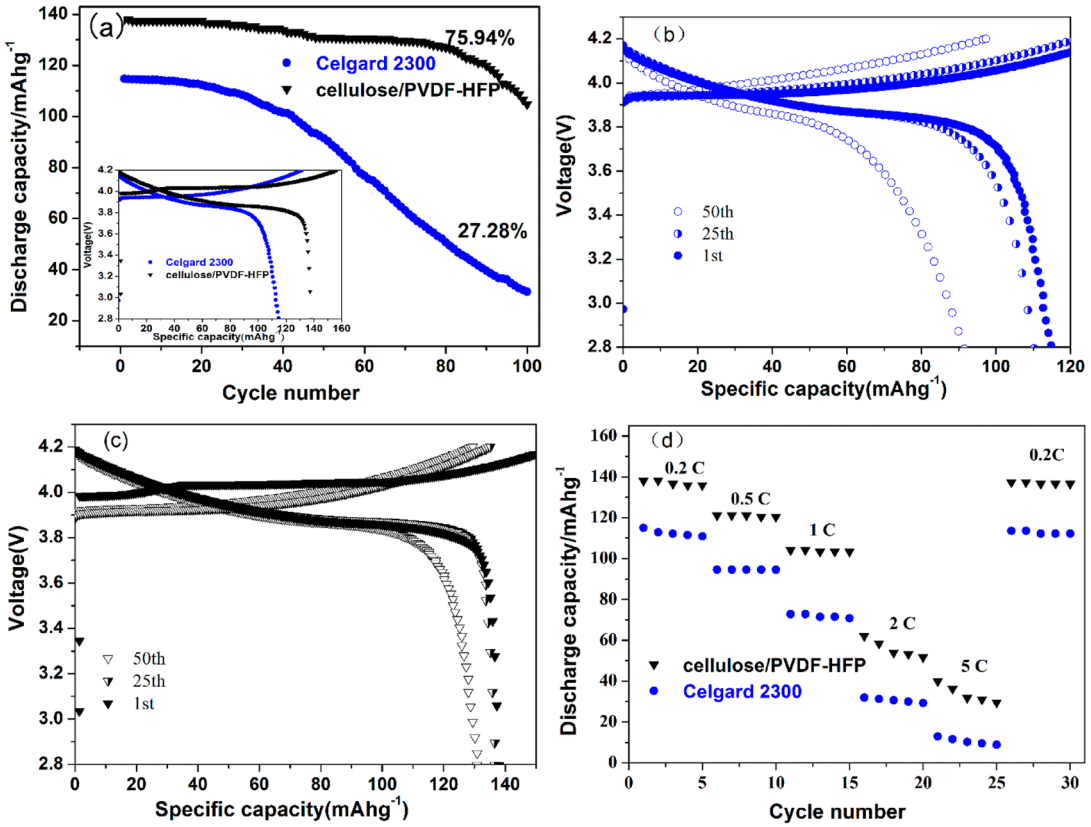


**Figure 6.** Cycle performance of the $LiCoO_2$ cells using Celgard 2300 and cellulose/PVDF-HFP separators (a), first charge and discharge curves (inset in panel a); 1st, 25th, and 50th charge and discharge curves for Celgard 2300 (b) and cellulose/PVDF-HFP separators (c); rate performance of cells using Celgard 2300 and cellulose/PVDF-HFP (d).

**Table 2. Discharge Capacity of Batteries Assembled with Various Separators**

| authors | materials | discharge rate (C) | discharge capacities ($mAh \cdot g^{-1}$) |
|---|---|---|---|
| this study | cellulose/PVDF-HFP (coaxial nanofiber) | 0.2 | 138.0 |
| Y. P. Wu et al.[25] | methyl cellulose | 0.2 | 130 |
| G. L. Cui et al.[26] | cellulose-based composite | 0.5 | 120 |
| P. Zhang et al.[27] | $SiO_2$−PMMA (core−shell) | 0.5 | 108 |
| Q. Xu et al.[4] | polydopamine-coated membrane | 0.2 | 131 |
| Y. S Zhu et al.[28] | PVDF/polyborate | 0.2 | 129.5 |
| S. Q. Wang et al.[29] | aluminum oxide | 0.2 | 113.8 |

coaxially electrospun cellulose/PVDF-HFP fibrous membrane is a very promising material for high performance and safe LIB separators.

## CONCLUSIONS

An environmentally friendly polymer material, cellulose acetate, was successfully extracted from waste cigarette filter tips and skillfully electrospun with PVDF-HFP into a coaxial core/shell composite nanofiber membrane. Following alkaline hydrolysis to convert cellulose acetate to cellulose, the membrane demonstrated a good mechanical property, superior flame retardancy, excellent thermal stability, and good electrolyte wettability. The ionic conductivity of the cellulose/PVDF-HFP separator was much higher than that of the commercial separator (Celgard 2300) saturated with liquid electrolyte. Moreover, cells assembled with a cellulose-based coaxial nanofiber separator exhibited high storage, better cycling, and enhanced rate performance compared to the battery using a commercial separator. All these results suggest that this composite nanofiber membrane from wasted cigarette filter tips would be a promising separator for high performance and safe lithium-ion batteries.

## AUTHOR INFORMATION

### Corresponding Author

*Qufu Wei. Tel.:+86-510-85912009. E-mail: qfwei@jiangnan.edu.cn.

### Notes

The authors declare no competing financial interest.

## ACKNOWLEDGMENTS

We are grateful for the financial support from the National Natural Science Foundation of China (51203064), Industry-Academia-Research Joint Innovation Fund of Jiangsu Province (BY2014023-4), and National High-tech R&D Program of China (863 Program 2012AA030313).



DOI: 10.1021/acssuschemeng.5b00032
ACS Sustainable Chem. Eng. 2015, 3, 932−940

## REFERENCES


(1) Kim, J. H.; Kim, J. H.; Choi, E. S.; Yu, H. K.; Kim, J. H.; Wu, Q. L.; Chun, S. J.; Lee, S. Y.; Lee, S. Y. Colloidal silica nanoparticle-assisted structural control of cellulose nanofiber paper separators for lithium-ion batteries. *J. Power Sources* **2013**, *242*, 533−540.

(2) Zuo, X.; Liu, X.-M.; Cai, F.; Yang, H.; Shen, X. D.; Liu, G. A novel all-solid electrolyte based on a co-polymer of poly-(methoxy/hexadecal-poly(ethylene glycol)methacrylate) for lithium-ion cell. *J. Mater. Chem.* **2012**, *22*, 22265−22271.

(3) Yanilmaz, M.; Meltem, D.; Zhang, X. W. Evaluation of electrospun $SiO_2$/nylon 6, 6 nanofiber membranes as a thermally-stable separator for lithium-ion batteries. *Electrochim. Acta* **2014**, *133*, 501−508.

(4) Goodenough, J. B.; Kim, Y. Challenges for rechargeable batteries. *J. Power Sources* **2011**, *196*, 6688−6694.

(5) Adsul, M. G.; Varma, A. J.; Gokhale, D. V. Lactic acid production from waste sugarcane bagasse derived cellulose. *Green Chem.* **2007**, *9*, 58−62.

(6) Zhang, H. P.; Liang, S. S.; Sun, B. P.; Yang, X. J.; Wu, X.; Yang, T. A hybrid redox flow battery with high energy efficiency using a low cost sandwiched membrane as a separator and $LiMn_2O_4$ as a cathode. *J. Mater. Chem. A* **2013**, *1*, 14476−14479.

(7) Zhang, X. Y.; Cheng, S. A.; Huang, X.; Logan, B. E. The use of nylon and glass fiber filter separators with different pore sizes in air-cathode single-chamber microbial fuel cells. *Energy Environ. Sci.* **2010**, *3*, 659−664.

(8) Zhang, S. S. A review on the separators of liquid electrolyte Li-ion batteries. *J. Power Sources* **2007**, *164*, 351−364.

(9) Arora, P.; Zhang, Z. M. Battery separators. *Chem. Rev.* **2004**, *104*, 4419−4462.

(10) Huang, X. S. Separator technologies for lithium-ion batteries. *J. Solid State Electrochem.* **2011**, *15*, 649−662.

(11) Deka, M.; Kumar, A. Electrical and electrochemical studies of poly(vinylidene fluoride)-clay nanocomposite gel polymer electrolytes for Li-ion batteries. *J. Power Sources.* **2011**, *196*, 1358−1364.

(12) Huang, F. L.; Wang, Q. Q.; Wei, Q. F.; Gao, W. D.; Shou, H. Y.; Jiang, S. D. Dynamic wettability and contact angles of poly(vinylidene fluoride) nanofiber membranes grafted with acrylic acid. *Express Polym. Lett.* **2010**, *9*, 551−558.

(13) Lalia, B. S.; Samad, Y. A.; Hashaikeh, R.; Appl, J. Nanocrystalline-cellulose-reinforced poly(vinylidenefluoride-co-hexafluoropropylene) nanocomposite films as a separator for lithium ion batteries. *Polym. Sci.* **2012**, *126*, E441−E447.

(14) Li, M. Y.; Katsouras, I.; Piliego, C.; Glasser, G.; Lieberwirth, I.; Blom, P. W. M.; de Leeuw, D. M. Controlling the microstructure of poly(vinylidene-fluoride) (PVDF) thin films for microelectronics. *J. Mater. Chem. C* **2013**, *1*, 7695−7702.

(15) Wei, W. P.; Zhang, H. M.; Li, X. F.; Zhang, H. Z.; Li, Y.; Vankelecom, I. Hydrophobic asymmetric ultrafiltration PVDF membranes: An alternative separator for VFB with excellent stability. *Phys. Chem. Chem. Phys.* **2013**, *15*, 1766−1771.

(16) Costa, C. M.; Silva, M. M.; Lanceros-Méndez, S. Battery separators based on vinylidene fluoride (VDF) polymers and copolymers for lithium ion battery applications. *RSC Adv.* **2013**, *3*, 11404−11417.

(17) Stephan, A. M. Review on gel polymer electrolytes for lithium batteries. *Eur. Polym. J.* **2006**, *42*, 21−42.

(18) Li, D. W.; Luo, L.; Pang, Z. Y.; Ding, L.; Wang, Q. Q.; Ke, H. Z.; Huang, F. L.; Wei, Q. F. Novel phenolic biosensor based on a magnetic polydopamine-laccase-nickel nanoparticle loaded carbon nanofiber composite. *ACS Appl. Mater. Interfaces* **2014**, *6*, 5144−5151.

(19) Huang, F. L.; Xu, Y. F.; Liao, S. Q.; Yang, D. W.; Hsieh, Y. L.; Wei, Q. F. Preparation of Amidoxime polyacrylonitrile chelating nanofibers and their application for adsorption of metal ions. *Materials* **2013**, *6*, 969−980.

(20) Wang, X.; He, T. T.; Li, D. W.; Huang, F. L.; Wei, Q. F.; Wang, X. L. Electromagnetic properties of hollow PAN/$Fe_3O_4$ composite nanofibres via coaxial electrospinning. *Int. J. Mater. Prod. Technol.* **2013**, *46*, 95−105.

(21) Xia, X.; Wang, X.; Zhou, H. M.; Liu, X.; Xue, L. G.; Zhang, X. W. The effects of electrospinning parameters on coaxial Sn/C nanofibers: Morphology and lithium storage performance. *Electrochim. Acta* **2014**, *121*, 345−351.

(22) Kumari, M.; Gupta, B.; IkKram, S. Characterization of N-isopropyl acrylamide/acrylic acid grafted polypropylene nonwoven fabric developed by radiation-induced graft polymerization. *Phys. Chem.* **2012**, *81*, 1729−1735.

(23) Wang, M. K.; Zhao, F.; Dong, S. J. A single ionic conductor based on Nafion and its electrochemical properties used as lithium polymer electrolyte. *J. Phys. Chem. B* **2004**, *108*, 1365−1370.

(24) Malathi, J.; Kumaravadivel, M.; Brahmanandhan, G. M.; Hema, M.; Baskaran, R.; Selvasekarapandian, S. Structural thermal and electrical properties of PVA−$LiCF_3SO_3$ polymer electrolyte. *J. Non-Cryst. Solids* **2010**, *356*, 2277−2281.

(25) Xiao, S. Y.; Wang, F. X.; Yang, Y. Q.; Chang, Z.; Wu, Y. P. An environmentally friendly and economic membrane based on cellulose as a gel polymer electrolyte for lithium ion batteries. *RSC Adv.* **2014**, *4*, 76−81.

(26) Zhu, Y. S.; Wang, F. X.; Liu, L. L.; Xiao, S. Y.; Chang, Z.; Wu, Y. P. Composite of a nonwoven fabric with poly(vinylidene fluoride) as a gel membrane of high safety for lithium ion battery. *Energy Environ. Sci.* **2013**, *6*, 618−624.

(27) Yang, P.; Zhang, P.; Shi, C.; Chen, L. X.; Dai, J. H.; Zhao, B. The functional separator coated with core-shell structured silica-poly(methyl methacrylate) sub-microspheres for lithium-ion batteries. *J. Membr. Sci.* **2015**, *474*, 148−155.

(28) Zhu, Y. S.; Xiao, S. Y.; Shi, Y.; Yang, Y.; Hou, Y. Y.; Wu, Y. P. A composite gel polymer electrolyte with high performance based on poly (vinylidene fluoride) and polyborate for lithium ion batteries. *Adv. Energy Mater.* **2014**, *6*, 7790−7797.

(29) Chen, J. J.; Wang, S. Q.; Ding, L. X.; Ding, Y. B.; Wang, H. H. Performance of through-hole anodic aluminum oxide membrane as a separator for lithium-ion battery. *J. Membr. Sci.* **2014**, *461*, 22−27.

(30) Zhang, J. J.; Yue, L. P.; Kong, Q. S.; Liu, Z. H.; Zhou, X. H.; Zhang, C. J.; Xu, Q.; Zhang, B.; Ding, G. L.; Qin, B. S.; Duan, Y. L.; Wang, Q. F.; Yao, J. H.; Cui, G. L.; Chen, L. Q. Sustainable, heat-resistant and flame-retardant cellulose-based composite separator for high-performance lithium ion battery. *Sci. Rep.* **2014**, *4*, 3935.




DOI: 10.1021/acssuschemeng.5b00032
*ACS Sustainable Chem. Eng.* 2015, 3, 932−940